



Short communication

## Determination of biotin following derivatization with 2-nitrophenylhydrazine by high-performance liquid chromatography with on-line UV detection and electrospray-ionization mass spectrometry

Chikako Yomota\*, Yukiko Ohnishi

*National Institute of Health Sciences, 1-18-1 Kamiyoga, Setagaya-ku, Tokyo 158-8501, Japan*

Received 7 February 2006; received in revised form 13 December 2006; accepted 15 December 2006

Available online 21 December 2006

### Abstract

Currently, biotin is typically determined in Japan using a microbiological method. Such microbiological assays are sensitive, but they are not always highly specific and are also rather tedious and time-consuming. In the present study, RP-HPLC and LC-MS methods for the determination of biotin have been developed by derivatizing the carboxyl group with 2-nitrophenylhydrazine hydrochloride. 2-Nitrophenylhydrazine is used for the derivatization of carboxylic acids, and these derivatives are known to be applicable to LC-MS detection. Biotin in tablets were extracted by the addition of water and ultrasonic agitation. In order to clean up the sample solution, the filtrate was applied to an ODS cartridge and eluted with methanol. The conditions for preparing the 2-nitrophenylhydrazide derivatives were modified from a previous report for fatty acids. Good recovery rates of over 70% were obtained for the addition of 5–125  $\mu\text{g}$  of biotin per formulation. The detection limit in HPLC at 400 nm was 0.6 ng per injection, with good linearity being obtained over the concentration range 0.001–0.2  $\mu\text{g}$  per injection. Further, derivatives were determined by LC-MS with electrospray ionization, where the spectra indicated the molecular ions  $[M + H]^+$ . The detection limit was 0.025 ng per injection in the selected ion monitoring analysis, and linearity was observed in the range of 0.6–6 ng per injection. The proposed method could be used to specifically determine the presence of biotin in relatively clean samples.

© 2006 Elsevier B.V. All rights reserved.

**Keywords:** Biotin; 2-Nitrophenylhydrazine derivative; HPLC; LC-MS; Electro spray ionization

### 1. Introduction

Biotin (vitamin H) is a coenzyme essential in amino acid metabolism and in the maintenance of skin, hair and nerves. Low biotin intake has been reported to result in serious biochemical disorders, such as reduced carboxylase activity, inhibition of protein and RNA synthesis and reduced antibody production. In recent years, the interest in this vitamin has increased, mainly due to diseases such as multiple carboxylase deficiency, which can be successfully treated by biotin administration. A decrease in biotin status has been reported to occur in several population groups, such as pregnant women.

In Japan, in 2001, the nutritional requirement of 30  $\mu\text{g}$  of biotin per day was set for adults and 5  $\mu\text{g}$  for infants, with an additional requirement of 5  $\mu\text{g}$  for pregnant women. Three years

later, biotin was also approved as a food additive and now can be supplied as ingredient in food with nutrient function claims [1].

Diagnosis of biotin deficiency is crucial as well as the monitoring of biotin levels in biological fluids of patients receiving biotin treatment. It is also important to determine biotin levels in pharmaceutical preparations as well as in food and food supplement products, which constitute the main source of biotin for humans. For this reason, analytical methods have been developed, in order to determine biotin in biological fluids, as well as in various types of food products and pharmaceutical preparations containing biotin [2].

Biotin has long been determined by a microbiological method, which is tedious and time-consuming [3]. Recently, various HPLC methods have been described to improve the selectivity [4–9]. Using 4-bromomethylmethoxycoumarin [4], 9-anthryldiazomethane (ADAMS) [5,6], and 1-pyrenyldiazomethane (PDAM) [7] as pre-column reagents, biotin was derivatized and determined by fluorometric detection. However

\* Corresponding author. Tel.: +81 3 3700 1141; fax: +81 3 3707 6950.

E-mail address: [yomota@nih.go.jp](mailto:yomota@nih.go.jp) (C. Yomota).

they are still inappropriate for common analysis, due to a lack of sensitivity or their complicated procedure or the many unknown peaks derived from reagents. Kamata et al. reported a method of applying electrochemical detection to determine biotin in multivitamin pharmaceutical preparations [8], and achieved a good separation. Further, biotin methylester was described as being well detected by MS detection in a positive ion chemical ionization mode [9]. Wolf et al., reported the quantification of biotin in human skin using LC–MS and resulted in the detection limit of 0.8 ng/mL [10]. Recently, LC–MS/MS analysis of biotin was also reported to be applicable to food samples with a biotin content over 100 µg/kg [11].

On the other hand, it was demonstrated in some reports that aliphatic acids and organic acids reacted selectively with 2-nitrophenylhydrazine hydrochloride (2-NPH·HCl), and produced derivatives that are UV detectable [12–15]. The main advantage of derivatization with hydrazines, using coupling reagent 1-ethyl-3-(3-dimethylaminopropyl)-carbodiimide hydrochloride (EDC·HCl), with respect to other derivatization reagents is that the reaction can be carried out under very mild conditions (weakly acidic medium at 60 °C) in an aqueous environment. Here, we report the reaction of 2-NPH·HCl for the determination of biotin in pharmaceutical products or food with nutrient function claims. For further improvement in detection specificity, LC–MS is also applied. As described by Saitoh and Gamoh [15], hydrazide derivatives of organic acids were successfully detected by LC–MS with electrospray ionization.

## 2. Experimental

### 2.1. Reagent solutions

2-NPH·HCl (Tokyo Kasei Kogyo, Tokyo, Japan) solutions (0.02 M) were prepared by dissolving the reagent in water. A EDC·HCl (Dojindo Laboratories, Kumamoto, Japan) solution (0.25 M) was prepared by dissolving the reagent in methanol. A fresh working solution of EDC was prepared daily, by mixing with an equal part of a solution of 2% pyridine in ethanol. A potassium hydroxide solution (15%, w/v) in water was also prepared. All the reagent solutions were stable for at least 3 months when kept below 5 °C. Biotin was commercially available from Wako Pure Chemicals (Osaka, Japan). All other chemicals were of analytical-reagent grade, and solvents were of HPLC quality. The ultra-pure water used for sample preparation was obtained from a Milli-Q purification system (Millipore, Bedford, MA, USA).

### 2.2. Samples

Samples used for the recovery tests were typical commercial foods with nutrient function claims. One food was in the form of a tablet containing seven kinds of vitamin such as vitamin B<sub>1</sub> (6 mg/tablet), vitamin B<sub>2</sub> (5 mg/tablet), vitamin B<sub>6</sub> (5 mg/tablet), vitamin B<sub>12</sub> (5 mg/tablet), niacin (8 mg/tablet), pantothenic acid (12 mg), folic acid (0.2 mg/tablet), but not biotin. The other food was a drink containing vitamin C (1000 mg/250 mL) as a nutrient, but not biotin.

### 2.3. Sample preparation

Tablets were finely powdered, with an amount corresponding to 40–200 µg being accurately weighed and added to 10 mL of water. The solution was sonicated for 10 min and centrifuged for 5 min at 10,000 rpm, followed by further filtration using a membrane filter (0.2 µm; Dismic-25CS, Toyo Roshi Kaisha, Tokyo, Japan). The beverage was used without pretreatment or was diluted with water to contain between 4 and 20 µg/mL of biotin. A Sep-Pak Plus tC18ENV cartridge (Waters) was conditioned by successively passing methanol (5 mL), and 5 mM tetrabutylammonium bromide (TBA) solution (5 mL). Five mL of the sample solution was mixed with 1 mL of 5 mM TBA solution and loaded in the pre-conditioned cartridge. The cartridges were then washed with 5 mL of 5 mM TBA solution to remove matrix interference and the analyte was then eluted with 2 mL of methanol. The eluant was transferred to a 2 mL volumetric flask and brought to exactly 2 mL with additional methanol.

A 100 µL aliquot of methanol eluant was added to a screw vial containing 200 µL of 250 mM EDC·HCl solution and 200 µL of 2% pyridine solution. After the addition of 200 µL of 20 mM NPH·HCl solution, the mixture was heated at 25 °C for 10 min. To remove the interfering materials, 100 µL of 15% potassium hydroxide solution was added, and a mixture thus obtained was further heated at 60 °C for 10 min and then cooled. The resulting hydrazide mixture was injected directly into the HPLC and LC–MS systems.

## 3. Instruments

### 3.1. HPLC apparatus and conditions

HPLC analyses were performed on an LC-10 series (Shimadzu, Kyoto, Japan) liquid chromatography system equipped with two LC-10ADvp pumps, an SPD-10AVvp spectrophotometric detector, an SPD-M10Avp photodiode array detector, and a SIL-10ADvp autosampler. Data processing was carried out with a Class-VP LC workstation. For the reversed-phase column, an L-column ODS (250 × 4.6 mm, I.D., 5 µm) (Chemical Evaluation and Research, Tokyo, Japan) and a TSK guardgel ODS-80Ts (15 × 3.2 mm, I.D.) (Toso, Tokyo, Japan) were used. The detection wavelength was set at 400 nm and the column temperature was maintained at 40 °C. The mobile phase was the mixture of 20 mM potassium dihydrogenphosphate (pH 4.5) and acetonitrile (75:25), with a flow rate of 1 mL/min. Injection volume was 10 µL.

### 3.2. LC–MS

LC–MS measurements were carried out with an LC-10 series liquid chromatography system, coupled to a LC–MS-2010 mass spectrometer, equipped with an electro spray ionization source (ESI) (Shimadzu, Kyoto, Japan).

For the LC–ESI<sup>+</sup>-MS a split system 1/4 was used to introduce the effluent into the ES. The probe voltage was held at +1.5 kV and the cone voltage was set to 10 V. The block heater

temperature was 200 °C and CDL temperature was 250 °C. The nebulizing gas flow was 1.5 L/min and the pressure of drying gas was maintained at 0.2 mPa. Mass spectra were acquired by scanning from  $m/z$  100 to 500 and data were processed using software. The separation was performed in a Capcell Pak C18 UG120 (250 × 2 mm, I.D.) (Shiseido, Tokyo, Japan) under chromatographic conditions of: 0.1 ml/min flow-rate, 1  $\mu$ l sample injection volume and a mixture of methanol and 5 mM ammonium acetate (1:1) as the mobile phase.

## 4. Results and discussion

### 4.1. Examination of derivatization conditions

Due to the weak chromophoric properties of biotin, resulting in relatively poor sensitivity and selectivity of detection, pre-column derivatization methods have been developed with HPLC, using the reagent 2-nitrophenylhydrazine hydrochloride (2-NPH·HCl) for the derivatization of carboxylic groups.

The reaction conditions were investigated following the reported method [12,13] in order to ensure the maximum derivatization of biotin. The structures of biotin and NPH ester of biotin were shown in Fig. 1. The condition of HPLC by UV detection was investigated following the method reported for the acid hydrazides of fatty acids [12]. The effect of the EDC·HCl concentration on the peak area was investigated, and there was little difference in HPLC peak area at 400 nm of products formed for EDC concentrations between 150 and 400 mM; therefore 250 mM of EDC·HCl was selected because it fell in the middle of this range. Peak area was not much affected by concentrations of pyridine from 1 to 4% (v/v). We selected 2% as a medium value within this wide range. The relationship between the peak area of the acid hydrazides and the concentration of 2-NPH·HCl showed little change between 15 and 30 mM, but concentrations greater than 40 mM showed a decrease in peak area.

The temperature of derivatization can be an important factor in the optimization process rate [12]; however, we found little difference in peak area between 20 and 30 °C after 10 min reaction time and as long as 50 min (Fig. 2). A higher temperature (60 °C) decreased peak area by approximately 20%. The peak area for biotin became more consistent after 10 min at 20–30 °C, which suggested that the derivatization was completed after 10 min. Thus, derivatization could be carried out at a room temperature of approximately 25 °C. The derivatives of biotin standard solutions were stable for at least 10 days when kept below 5 °C. However, the sample solutions purified from tablets through cartridges were often unstable. For example, the peak area decreased to 80% if purified sample solutions

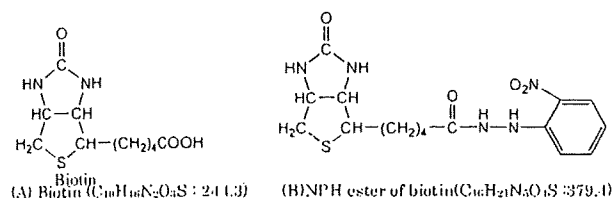


Fig. 1. Chemical structures of biotin (A) and NPH ester of biotin (B).

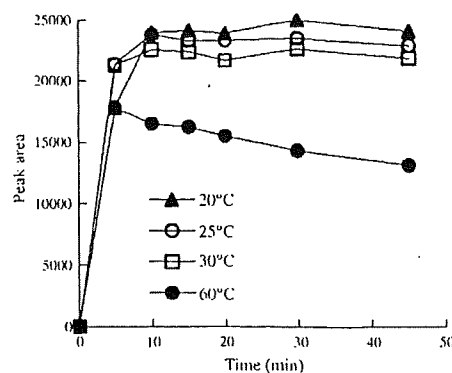


Fig. 2. Optimization of reaction time and reaction temperature for ester formation. A temperature of 25–50 °C had little effect on product formation between 10 and 50 min, whereas 60 °C reduced the total product formed by about 20%, and the reduction was greater with longer times.

stood for 3 h before derivatization. Therefore, the sample solutions should be converted immediately after preparation to the derivative.

### 4.2. HPLC separation and precision

Following the method described for the acid hydrazides of fatty acids [12], good chromatograms were obtained on reversed-phase columns using the mixture of 20 mM potassium dihydrogenphosphate (pH 4.5) and acetonitrile (75:25) as an eluent (Fig. 3A). The calibration curves were linear over the range 0.001–0.2  $\mu$ g per injection (eight levels, three replicates, intercept; –691.56, slope; 41699,  $r = 0.999$ ) and the relative standard deviation of peak areas of 0.06  $\mu$ g per injection ( $n = 6$ ) was 1.2%.

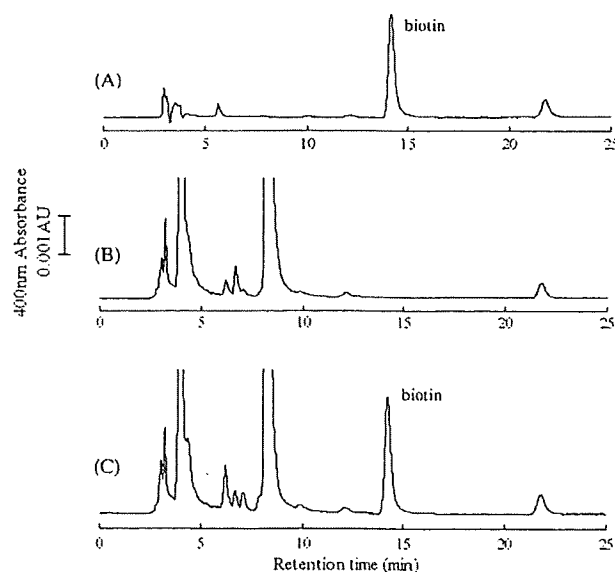


Fig. 3. HPLC chromatograms of tablet formulations: (A) standard solution of biotin NPH derivative (30  $\mu$ g/mL), (B) tablet with no added biotin, (C) tablet with added biotin at 120  $\mu$ g/tablet. Conditions: column, L-column (250 mm × 4.6 mm, I.D.); eluent, 20 mM potassium dihydrogenphosphate (pH 4.5) and acetonitrile (75:25); flow-rate, 1.0 mL/min; detection, UV at 400 nm; injection volume, 10  $\mu$ L.

Table 1  
Recovery tests of biotin with HPLC ( $n = 6$ )

	Amounts of added biotin	Recovery (%)
Standard solutions	5 $\mu\text{g/ml}$	97.7 $\pm$ 1.4
	50 $\mu\text{g/ml}$	103.2 $\pm$ 2.3
Products		
	Tablet	120 $\mu\text{g/tablet}$
Drink	5 $\mu\text{g/ml}$	73.3 $\pm$ 2.1

With HPLC, the detection limit was calculated to be 0.6 ng per injection ( $S/N = 3$ ,  $n = 6$ ), on the basis of  $S/N$  ratios.

#### 4.3. Recovery test

Recovery testing was investigated using two products: a tablet and a drink, which contained several vitamins other than biotin. The results of recovery test were summarized in Table 1.

Satisfactory recoveries, ranging from 97.7 to 103.2%, were obtained when the whole procedure was performed at two levels of standard solutions, 5 and 50  $\mu\text{g/mL}$ , respectively. The recoveries from the tablet, using HPLC after adding 120  $\mu\text{g}$  biotin per tablet, are 93.0%. In the case of the drink, 73.3% was obtained when 5  $\mu\text{g}$  of biotin was added per mL of the drink. HPLC chromatograms obtained for the recovery test from the tablet are shown in Fig. 3. Fig. 3A is the chromatogram for the standard solution of biotin NPH derivative and Fig. 3B is that for the tablet with no added biotin. As shown in Fig. 3C, the peaks for biotin were well separated from other large peaks and the peaks derived from the reagents were not distinctly observed. In many other derivatization methods such as fluorometric detection, there is a difficulty to spend too long analytical time to elute completely the large reagent peaks after a biotin peak. In this analytical procedure, other carboxylic vitamins, such as nicotinic acid, pantothenic acid and folic acid, were also detected as their derivatives. Their retention times in the same chromatographic conditions as Fig. 3C were confirmed by injecting each standard solution separately to be 12.7 min for nicotinic acid, 4 and 8 min for pantothenic acid, 4 and 4.4 min for folic acid. Folic acid may produce two derivatives due to its two carboxylic residues. However, in case of pantothenic acid, the reason for elution in two peaks was not clear. In Fig. 3B and C, the large peaks near 4 and 8 min may be derived from pantothenic acid contained in tablets.

The precision of the method was validated by both intra-day and inter-day variances in the case of the recoveries from the tablet. To determine intra-day variance, the assays were carried out five times in a day. Inter-day variance was determined by analyzing the samples over three days. From these results, the repeatability was 1.5% and intermediate precision was 2.5%. The limit of quantification was 2  $\mu\text{g/mL}$  as the initial sample solutions before the step of purification by Sep-Pak cartridges.

#### 4.4. Confirmation test with LC–MS

In analyzing the sample solutions extracted from tablets by HPLC, sometimes the interference peak appeared near the biotin

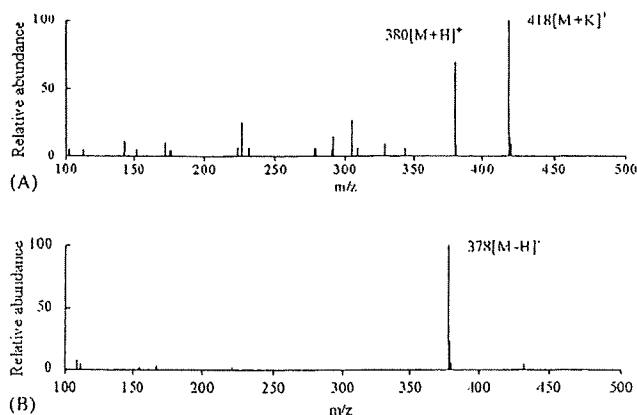


Fig. 4. LC–MS (ESI) spectra of NPH derivatives of biotin: (A) positive ion spectrum with molecular-related ions at  $m/z$  380 and the potassium-loaded ion at  $m/z$  418, (B) negative ion spectrum with the molecular-related ion at  $m/z$  378.

peak. Therefore, for a confirmation test, the MS detection was adopted. In the analysis of biotin derivatives by LC–MS, using ESI in both the positive and negative mode, a high sensitivity was achieved using the mobile phase of 5 mM ammonium acetate/methanol (1:1) solution. The positive and negative mass spectra of 2-NPH derivatives of biotin showed, not only molecular related ions ( $[M + H]^+$  ( $m/z$  380) and  $[M - H]^-$  ( $m/z$  378)), but also an  $m/z$  418, potassium-loaded ion in positive mode. (Fig. 4A and B). The calibration curves of the selected ion monitoring (SIM) chromatograms of  $[M + H]^+$  ( $m/z$  380), were linear over the range 0.6–6 ng per injection (six levels, three replicates, intercept; 12097, slope; 19735,  $r = 0.9996$ ) and the relative standard deviation of peak areas of 6 ng/injection ( $n = 6$ ) and also 0.6 ng per injection ( $n = 6$ ) were less than 2%. The detection limit of biotin derivative in LC–MS was calculated to be 0.025 ng per injection ( $S/N = 3$ ,  $n = 6$ ). Applying the SIM chromatograms, acceptable recoveries of 97.5  $\pm$  3.2% ( $n = 6$ ) were obtained for tablets without any other peak. These results showed that 2-NPH derivatives of biotin can be well identified with ESI-MS detection.

#### 5. Conclusion

Biotin can be selectively analyzed in an aqueous environment by derivatization with 2-NPH with UV-detection. Biotin derivatives can also be easily identified with LC–MS with ESI. From these results, this reaction appeared to be specific for the determination of as little as 0.6 ng of biotin, in the presence of large quantities of other substances. The proposed method could be used to specifically determine the presence of biotin in supplements and in pharmaceutical preparations.

#### References

- [1] Japan Food Additives Association: Japan's Specifications and Standards for Food Additives, Tokyo, 2006.
- [2] Analytical Methods for Food Additives in Food, Nihon Shokuhin Eisei Kyokai, Tokyo, 2000, p. 230.
- [3] E. Livaniou, D. Costopoulou, I. Vassiliadou, L. Leondiadis, J.O. Nyalala, D.S. Ithakissios, G.P. Evangelatos, J. Chromatogr. A 881 (2000) 331.

- [4] P.L. Desbene, S. Coustal, F. Frappier, *Anal. Biochem.* 128 (1983) 359.
- [5] Y. Kanazawa, T. Nakano, H. Tanaka, *NIPPON KAGAKU KAISHI* 3 (1984) 434.
- [6] K. Hayakawa, J. Oizumi, *J. Chromatogr.* 413 (1987) 247.
- [7] T. Yoshida, A. Uetake, C. Nakai, N. Nimura, T. Kinoshita, *J. Chromatogr.* 456 (1988) 421.
- [8] K. Kamata, T. Hagiwara, M. Takahashi, S. Uehara, K. Nakayama, K. Akiyama, *J. Chromatogr.* 356 (1986) 326.
- [9] M. Azoulay, P.L. Desbene, F. Frappier, *J. Chromatogr.* 303 (1984) 272.
- [10] R. Wolf, C. Huschka, K. Raith, W. Wohlab, R. Neubert, *Anal. Commun.* 34 (1997) 355.
- [11] U. Höller, F. Wachter, C. Wehrli, C. Fizez, *J. Chromatogr. B* 831 (2006) 8.
- [12] H. Miwa, C. Hiyama, M. Yamamoto, *J. Chromatogr.* 321 (1985) 165.
- [13] H. Miwa, *J. Chromatogr. A* 881 (2000) 365.
- [14] R. Peters, J. Hellenband, Y. Mengerink, A. Ven der Wal, *J. Chromatogr. A* 1031 (2004) 35.
- [15] H. Saitoh, K. Gamoh, *BUNSEKI KAGAKU* 52 (2003) 923.

## Inhibition of Mannitol Crystallization in Frozen Solutions by Sodium Phosphates and Citrates

Ken-ichi Izutsu,\* Chikako YOMOTA, and Nobuo AOYAGI

National Institute of Health Sciences; 1-18-1 Kamiyoga, Setagaya-ku, Tokyo 158-8501, Japan.

Received November 10, 2006; accepted January 15, 2007; published online January 19, 2007

Effects of co-solutes on the physical property of mannitol and sorbitol in frozen solutions and freeze-dried solids were studied as a model of controlling component crystallinity in pharmaceutical formulations. A frozen mannitol solution (500 mM) showed a eutectic crystallization exotherm at  $-22.8^{\circ}\text{C}$ , whereas sorbitol remained amorphous in the freeze-concentrated fraction in the thermal scan. Various inorganic salts reduced the eutectic mannitol crystallization peak. Trisodium and tripotassium phosphates or citrates prevented the mannitol crystallization at much lower concentrations than other salts. They also raised transition temperatures of the frozen mannitol and sorbitol solutions ( $T_g'$ : glass transition temperature of maximally freeze-concentrated amorphous phase). Crystallization of some salts (e.g., NaCl) induced crystallization of mannitol at above certain salt concentration ratios. Thermal and near-infrared analyses of cooled-melt amorphous sorbitol solids indicated increased intermolecular hydrogen-bonding in the presence of trisodium phosphate. The sodium phosphates and citrates should prevent crystallization of mannitol in frozen solutions and freeze-dried solids by the intense hydrogen-bonding and reduced molecular mobility in the amorphous phase.

**Key words** amorphous; crystallization; formulation; freeze-drying; thermal analysis

Active ingredients and excipients in pharmaceutical solid formulations are in the amorphous or crystalline states. Application of amorphous solids is receiving increasing attention because of the unique physical and functional properties (e.g., higher dissolution rate, stabilization of freeze-dried proteins).<sup>1–4</sup> Controlling the component crystallinity through optimizing the compositions and the manufacturing process (freeze-drying, quench cooling of hot-melt liquids) is a relevant method in formulation development because each ingredient and excipient possess different intrinsic propensity for crystallization.<sup>5–7</sup> Freeze-drying with a large amount of “inert” nonionic molecules (e.g., disaccharides, soluble polymers) that are likely to form amorphous solid, is a popular way to obtain the intrinsically crystallizing ingredient in the non-crystalline dispersed state. The method, however, has some limitations in terms of the applicable excipients and the physical properties of the resulting solids.<sup>8</sup> Various inorganic salts also prevent crystallization of other solutes in frozen solutions and freeze-drying processes through mixing and/or complex formation.<sup>9–11</sup>

Mannitol is a popular excipient that tends to crystallize in frozen aqueous solutions.<sup>12</sup> The superior cake appearance and physical stability of the crystalline freeze-dried solids make mannitol a good bulking agent for many parenteral formulations of low-molecular-weight pharmaceuticals. The crystallization process of mannitol in frozen solutions, the resulting crystal polymorphs, and the effect of co-solutes on the physical properties have been studied extensively as models to elucidate the component crystallization process in multi-solute systems.<sup>13–19</sup> Co-lyophilization with sucrose prevents crystallization of mannitol during freeze-drying at sucrose/mannitol weight concentration ratios above 2–3.<sup>8,20,21</sup> Some salts (e.g., NaCl) that possess high melt miscibility with mannitol prevent its crystallization in frozen solutions at much lower concentrations than sucrose, whereas the low transition temperatures ( $T_g'$ : glass transition temperature of the maximally freeze-concentrated amorphous phase) of

the frozen solutions make it difficult to freeze-dry without physical collapse.<sup>9,12,22</sup>

Reduction of molecular mobility in the freeze-concentrated phase is another approach to obtain amorphous freeze-dried solids. Some salts (e.g., sodium tetraborate, boric acid) that effectively raise  $T_g'$ s of frozen polyol solutions (e.g., saccharides, sugar alcohols) by complex formation would prevent spatial rearrangement of the mannitol molecules required for crystallization.<sup>23–25</sup> Recent studies showed that some pH-adjusting excipients (e.g., sodium phosphate buffer) also raise glass transition temperature ( $T_g$ ) of amorphous freeze-dried saccharides.<sup>26,27</sup> Some phosphate salts also prevent crystallization of mannitol during freeze-drying processes, suggesting contribution of the reduced molecular mobility in the amorphous mixture.<sup>3,22,28</sup> The purpose of this study was to elucidate the effect of phosphate and citrate salts on the physical properties of mannitol and sorbitol in the frozen aqueous solutions and in the dried solids. Different intrinsic tendency of mannitol and its isomer (sorbitol) for crystallization provided information on the mechanisms and requirements to obtain the stable amorphous solids. Controlling the component crystallinity by the widely used excipients should be of practical importance in developing formulations without particular safety concerns.

### Experimental

**Materials** All the proteins and other chemicals employed in this study were of analytical grade and obtained from the following commercial sources: sucrose (Sigma-Aldrich, St. Louis, MO, U.S.A.); trisodium phosphate  $\cdot 12\text{H}_2\text{O}$  (Katayama Chemical, Osaka, Japan); disodium hydrogen citrate and sodium dihydrogen citrate (Kanto Chemical, Tokyo, Japan); D(+)-mannitol, D-sorbitol, and other chemicals (Wako Pure Chemical, Osaka).

**Freeze-Drying and Preparation of Amorphous Solids** Aqueous solutions (250  $\mu\text{l}$ ) containing 500 mM mannitol and various concentrations of co-solutes in flat-bottom glass vials (10 mm diameter) were lyophilized using a freeze-drier (Freezevac 1C; Tozai Tsusho, Tokyo). The solutions were frozen by immersion in liquid nitrogen, transferred to the shelf of the freeze-dryer, and lyophilized without a shelf temperature control for 12 h and at  $35^{\circ}\text{C}$  for 4 h. The solids were applied for the thermal analysis within 48 h of the preparation. Mixed powders containing sorbitol (approx. 200 mg), salt, and

\* To whom correspondence should be addressed. e-mail: izutsu@nihs.go.jp

aliquot of water (50  $\mu$ l) in crystal cuvettes or glass tubes were heated under vacuum at 160  $^{\circ}$ C for 20 min using a drying oven (DP23, Yamato Scientific Inc., Tokyo), then cooled at room temperature to prepare amorphous solids for thermal and spectroscopic analyses.

**Thermal Analysis** Thermal analyses of frozen solutions and freeze-dried solids were performed using a differential scanning calorimeter (DSC-Q10; TA Instruments, New Castle, DE, U.S.A.) with an electric refrigerating system and associated software (Universal Analysis). Indium and cyclohexane were used for the DSC calibration. Aliquots of solutions (10  $\mu$ l) in aluminum cells were scanned from  $-70^{\circ}$ C at  $5^{\circ}$ C/min after the system had been cooled at  $-10^{\circ}$ C/min to study the thermal profile of the frozen solutions. The effect of a heat treatment (annealing) on the thermal properties of the frozen solutions was studied after the initial heating scan was paused at  $-10^{\circ}$ C, and then the samples were maintained at the temperature for 30 min. Thermal data were acquired in the subsequent heating scan from  $-70^{\circ}$ C at  $5^{\circ}$ C/min. The extent of mannitol crystallization exotherm was obtained from the peak area under the baseline of the heat flow. Peaks in the derivative thermograms were assigned to glass transition temperatures of the maximally freeze-concentrated amorphous phases ( $T_g$ 's). Thermal analyses of the freeze-dried solids (1.7–2.2 mg) were performed from  $-30^{\circ}$ C at  $10^{\circ}$ C/min. The cooled-melt solids (approx. 5 mg) were scanned from  $-30^{\circ}$ C at  $5^{\circ}$ C/min.

**Near-Infrared Spectroscopy** Near-infrared analysis was performed using a FT-NIR system (MPA, Bruker Optik GmbH, Germany) with OPUS software. Absorbance of the sample (1-mm light path length) at 4000 to 12000  $\text{cm}^{-1}$  range was obtained at room temperature (25  $^{\circ}$ C) with a  $2 \text{ cm}^{-1}$  resolution in 128 scans.

## Results

Figure 1 shows thermograms of frozen solutions containing an identical concentration (500 mM) of various solutes. Frozen citric acid and sodium citrate solutions showed ther-

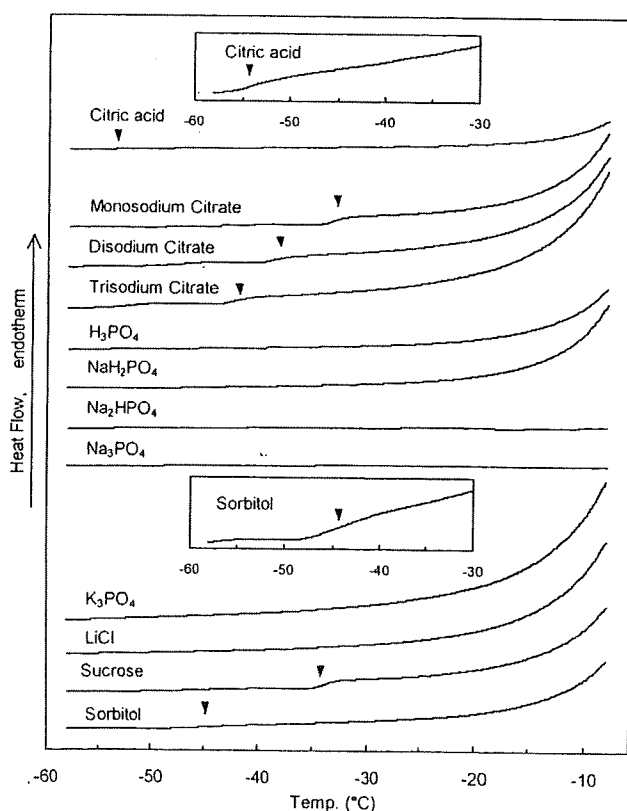


Fig. 1. Thermal Profiles of Frozen Single-Solute Aqueous Solutions (500 mM, 10  $\mu$ l) Scanned from  $-70^{\circ}$ C at  $5^{\circ}$ C/min

Glass transition temperatures of the maximally freeze-concentrated amorphous phases ( $T_g$ 's) are marked with reversed triangles ( $\blacktriangledown$ ).

mograms typical for amorphous supercooled freeze-concentrated phase, with the baseline shifts ( $T_g$ 's) at  $-53.4^{\circ}$ C (citric acid),  $-33.4^{\circ}$ C (sodium dihydrogen citrate),  $-38.8^{\circ}$ C (disodium hydrogen citrate), and  $-42.5^{\circ}$ C (trisodium citrate).<sup>29</sup> The transitions ( $T_g$ 's) of frozen sucrose and sorbitol solutions were observed at  $-33.8^{\circ}$ C and  $-44.2^{\circ}$ C, respectively. Some other frozen solutions (500 mM  $\text{H}_3\text{PO}_4$ ,  $\text{NaH}_2\text{PO}_4$ ,  $\text{K}_3\text{PO}_4$ ,  $\text{LiCl}$ ) showed a gradual shift of the thermogram baseline that suggested an amorphous freeze-concentrated phase with  $T_g$  below  $-55^{\circ}$ C. Freezing of aqueous solutions containing di- and trisodium phosphate ( $\text{Na}_2\text{HPO}_4$ ,  $\text{Na}_3\text{PO}_4$ ) solutions showed endotherm peaks in the cooling process (data not shown) and flat thermograms in the heating scan, indicating that the salt crystallization was completed before the heating scan.<sup>5,30</sup> Some frozen salt solutions showed endotherm peaks that indicated eutectic crystal melting at  $-19.8^{\circ}$ C ( $\text{NaCl}$ ),  $-8.9^{\circ}$ C ( $\text{KCl}$ ), and  $-14.2^{\circ}$ C ( $\text{RbCl}$ ) (data not shown). The peak temperatures were slightly (approx.  $2^{\circ}$ C) higher than the values in some literature probably because of the higher scanning rate in this study.<sup>5,6,31</sup>

Figure 2 shows DSC scans of frozen solutions containing 500 mM mannitol (approx. 91.1 mg/ml) and varied concentrations of sodium hydrogen phosphates ( $\text{Na}_2\text{HPO}_4$ ,  $\text{NaH}_2\text{PO}_4$ ,  $\text{Na}_3\text{PO}_4$ ) in the first heating scan from  $-70^{\circ}$ C, and in the second heating scan after a heat treatment (annealing) at  $-10^{\circ}$ C for 30 min. The frozen mannitol solution showed a large eutectic crystallization exotherm peak at  $-22.8^{\circ}$ C in the first scan. Several smaller thermal events, including two possible  $T_g$ 's ( $T_{g1}$ :  $-37.5^{\circ}$ C,  $T_{g2}$ :  $-29.0^{\circ}$ C) and a small endotherm ( $-24.3^{\circ}$ C), were also observed prior to the crystallization exotherm.<sup>17,21,28</sup> A small exotherm peak that suggests partial crystallization was observed in the cooling process of some frozen mannitol solutions (data not shown). The second scan of the frozen mannitol solution after the

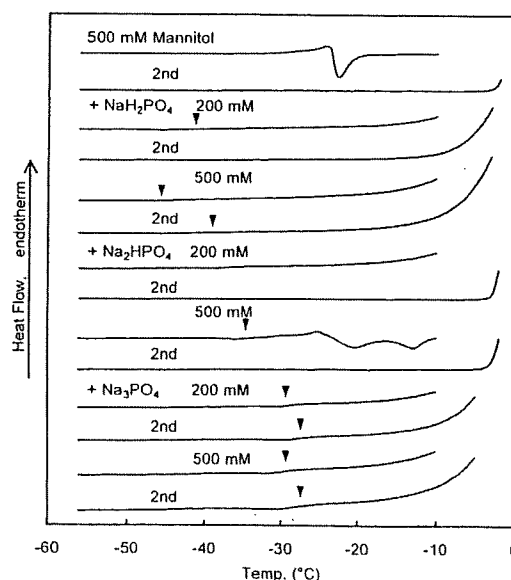


Fig. 2. Thermal Profiles of Frozen Solutions Containing Mannitol (500 mM) and Varied Concentrations of Sodium Phosphates in the First Scan from  $-70^{\circ}$ C at  $5^{\circ}$ C/min (Upper) and the Second Scan after a Heat Treatment at  $-10^{\circ}$ C for 30 min

The glass transitions ( $T_g$ 's) are marked with reversed triangles ( $\blacktriangledown$ ).

heat treatment resulted in a flat thermogram up to the ice-melting temperature, indicating the crystallized mannitol in the frozen solution.

The phosphate salts showed varied effects on the thermal property of the frozen mannitol solution. The mannitol crystallization exotherm peak disappeared in the presence of  $\text{NaH}_2\text{PO}_4$  (200, 500 mM),  $\text{Na}_2\text{HPO}_4$  (200 mM) or  $\text{Na}_3\text{PO}_4$  (200, 500 mM), presenting a thermal transition ( $T'_g$ ) that indicated the amorphous freeze-concentrated phase surrounding ice crystals. The frozen solution containing 500 mM mannitol and 500 mM  $\text{Na}_2\text{HPO}_4$  showed two exotherm peaks that suggest crystallization of mannitol ( $-20.3^\circ\text{C}$ ) and  $\text{Na}_2\text{HPO}_4$  ( $-12.8^\circ\text{C}$ ). The second scan of frozen solutions containing mannitol and  $\text{NaH}_2\text{PO}_4$  (500 mM) or  $\text{Na}_3\text{PO}_4$  (200, 500 mM) also showed the  $T'_g$  transitions. A slight shift of the transition temperature ( $T'_g$ ) in the second scan suggested retention of the amorphous freeze-concentrated phase and some re-ordering (e.g., further ice crystal growth) of the frozen solution during the heat treatment.<sup>17)</sup> The second scan of frozen solutions containing mannitol and  $\text{Na}_2\text{HPO}_4$  (200, 500 mM) showed flat thermograms up to the ice-melting temperature, indicating the crystallized mannitol and the salt.<sup>18)</sup>

Figures 3 and 4 show effects of various co-solutes (e.g., phosphate, citrate, chloride salts) on the mannitol crystallization exotherm size and transition temperatures ( $T'_g$ 's) of the frozen solutions. The crystallization exotherm of the frozen mannitol solution (500 mM) was  $14.1 \pm 1.2 \text{ J/g}$  ( $n=3$ ). Most of

the solutes, except  $\text{H}_3\text{PO}_4$ , apparently reduced the mannitol crystallization peak concomitantly with the upward shift of the peak temperature. Alkali-metal chloride salts with smaller cations ( $\text{LiCl}$ ,  $\text{NaCl}$ ) were more effective at reducing the mannitol crystallization peak than those with larger cations ( $\text{KCl}$ ,  $\text{RbCl}$ ). The mannitol crystallization peak also disappeared in the presence of 200 mM sucrose or 150 mM  $\text{CH}_3\text{COONa}$ , indicating the prominent effect of the salts, especially compared in their weight concentrations. Addition of some solutes slightly increased the exotherm at lower concentrations (<100 mM), probably because they alter thermal transitions prior to the crystallization peak. Sodium and potassium phosphates showed varied ability to reduce the mannitol crystallization peak depending on the ionic valencies. The mannitol crystallization peak disappeared at different phosphate salt concentrations ( $\text{Na}_3\text{PO}_4$ ,  $\text{K}_3\text{PO}_4 < \text{Na}_2\text{HPO}_4$ ,  $\text{K}_2\text{HPO}_4 < \text{NaH}_2\text{PO}_4 < \text{KH}_2\text{PO}_4$ ). Sodium phosphate buffers containing both  $\text{NaH}_2\text{PO}_4$  and  $\text{Na}_2\text{HPO}_4$  at different concentration ratios (3:1, 1:1, and 1:3) showed the crystallization-preventing effects intermediate between those of the individual salt solutions (data not shown). The mannitol crystallization peak also disappeared at different sodium citrate and citric acid concentrations (trisodium citrate < disodium citrate < monosodium citrate < citric acid). The pronounced effect of tri- and divalent salts suggests the significance of ion concentrations or alkaline pH on the ability of co-solutes to prevent the mannitol crystallization. The mannitol crystallization peak re-appeared upon further addition of some salts (300–500 mM  $\text{Na}_2\text{HPO}_4$ , 500 mM  $\text{RbCl}$ ,

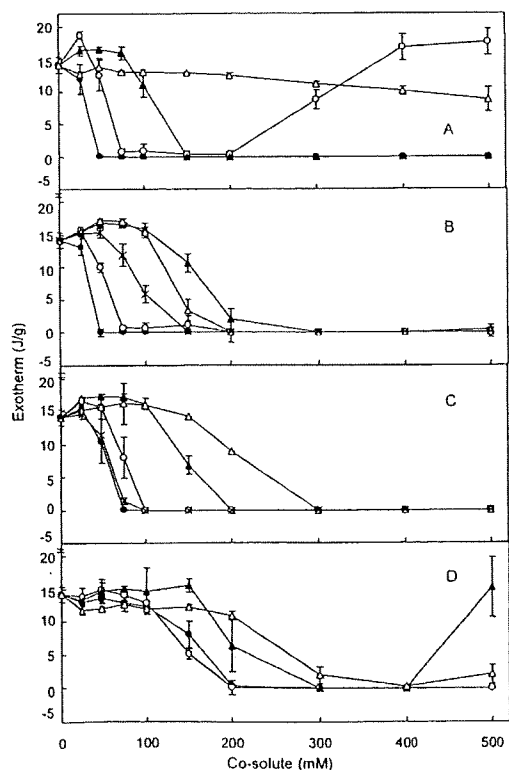


Fig. 3. Effects of Co-solutes on the Mannitol Crystallization Exotherm in Frozen Aqueous Solutions (10  $\mu\text{l}$ ) Scanned from  $-70^\circ\text{C}$  at  $5^\circ\text{C}/\text{min}$

The symbols denote frozen solutions containing (A) ●:  $\text{Na}_3\text{PO}_4$ , ○:  $\text{Na}_2\text{HPO}_4$ , ▲:  $\text{NaH}_2\text{PO}_4$ , △:  $\text{H}_3\text{PO}_4$ , (B) ●:  $\text{K}_3\text{PO}_4$ , ○:  $\text{K}_2\text{HPO}_4$ , ▲:  $\text{KH}_2\text{PO}_4$ , △: sucrose, ×:  $\text{CH}_3\text{COONa}$ , (C) ●: trisodium citrate, ○: disodium citrate, ▲: monosodium citrate, △: citric acid, ×: tripotassium citrate, (D) ●:  $\text{LiCl}$ , ○:  $\text{NaCl}$ , ▲:  $\text{KCl}$ , △:  $\text{RbCl}$  (mean value  $\pm$  S.D.,  $n=3$ ).

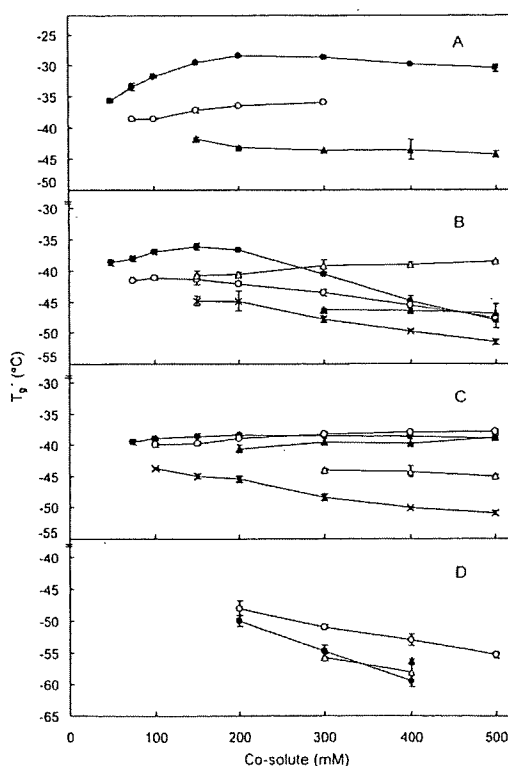


Fig. 4. Thermal Transition Temperatures ( $T'_g$ : Glass Transition of the Maximally Freeze-Concentrated Amorphous Phases) of the Frozen Solutions (10  $\mu\text{l}$ ) Containing Mannitol (500 mM) and Various Concentrations of Co-solutes Scanned from  $-70^\circ\text{C}$  at  $5^\circ\text{C}/\text{min}$

Symbols denote the co-solutes shown in Fig. 3 (mean value  $\pm$  S.D.,  $n=3$ ).



500 mM KCl). Crystallization of these salts in the single-solute frozen solutions (Fig. 1) suggested that the salt crystallization at high salt/mannitol ratio induced the mannitol crystallization in the remaining phase.

Frozen solutions containing the amorphous state mannitol and co-solute combinations showed apparent  $T'_g$  transition (Fig. 4). Extrapolating the transition temperatures of these mixture solutions suggested that  $T'_g$  of the frozen single-solute mannitol solution occurred at approximately  $-40^\circ\text{C}$ , which should correspond to the reported lower-temperature transition ( $T'_{g1}$ ).<sup>21,28</sup> Addition of some salts (e.g.,  $\text{NaH}_2\text{PO}_4$ ,  $\text{CH}_3\text{COONa}$ ,  $\text{LiCl}$ ,  $\text{NaCl}$ ,  $\text{KCl}$ ,  $\text{RbCl}$ ) lowered the transition temperature linearly depending on their concentrations. Sucrose slightly shifted the transition toward its intrinsic  $T'_g$  ( $-33.8^\circ\text{C}$ , Fig. 1).<sup>21</sup> These findings suggest simple mixing of the solutes in the freeze-concentrated phase, which transition temperature depends on the  $T'_g$ s of the individual components and their concentration ratios. In contrast, some phosphate and citrate salts non-linearly raised the transition temperature. Frozen solutions containing mannitol and trisodium or tripotassium salts ( $\text{Na}_3\text{PO}_4$ ,  $\text{K}_3\text{PO}_4$ , trisodium citrate) showed the highest transition temperatures at certain (150–300 mM) co-solute concentrations. The transition temperatures above those of the individual solutes (e.g., trisodium citrate:  $-42.5^\circ\text{C}$ ) suggested reduced molecular mobility in the freeze-concentrated phase.

Sorbitol remained amorphous in the single-solute (500 mM) frozen solution, presenting a  $T'_g$  transition at  $-44.2^\circ\text{C}$  (Fig. 1). Effect of the salts on the transition temperature of the frozen sorbitol solution ( $T'_g$ , Fig. 5) showed similar trends with the mannitol-salt systems. The non-linear upward shift of  $T'_g$ s suggested some interaction between the  $\text{Na}_3\text{PO}_4$  and the sugar alcohols, or altered environment in the freeze-concentrated phase. A salt crystallization exotherm peak was observed in the solutions containing 500 mM sorbitol and 300–500 mM  $\text{Na}_2\text{HPO}_4$ . Addition of 500 mM  $\text{Na}_2\text{HPO}_4$  resulted in low  $T'_g$  ( $-45.0^\circ\text{C}$ ) that suggested transition of phase-separated sorbitol fraction.

Effects of sodium phosphates and citrates on the physical properties of freeze-dried mannitol was studied (Fig. 6). Freeze-drying of mannitol resulted in  $\alpha$  or  $\beta$  polymorph crystal that showed a large crystal melting endotherm at approximately  $170^\circ\text{C}$ .<sup>18,32</sup> Co-lyophilization with the phosphate and citrate salts resulted in the small crystal melting peaks that suggested lower crystallinity or different polymorph (e.g.,  $\delta$ -form) in the solid.<sup>9,18,32</sup> Some solids showed glass transitions ( $35$ – $55^\circ\text{C}$ ), exotherm peaks of putative mannitol crystallization ( $60$ – $80^\circ\text{C}$ ), and small mannitol crystal melting peaks ( $150$ – $170^\circ\text{C}$ ). Transition temperatures ( $T_g$ s) of these co-lyophilized solids were higher than the reported  $T_g$  of amorphous mannitol (approx.  $13^\circ\text{C}$ ).<sup>33</sup> Freeze-dried solids containing mannitol and trisodium phosphate or citrate showed  $T_g$ s ( $52.9$ ,  $43.7^\circ\text{C}$ ) higher than those of the corresponding disodium salts ( $44.5$ ,  $40.0^\circ\text{C}$ ). Co-lyophilization with a higher concentration ( $200\text{ mM}$ ) of the co-solutes further reduced the mannitol crystallization during the process (data not shown). The upper shift of the glass transition temperature ( $T_g$ ) suggested altered interaction (e.g., hydrogen-bonding) between mannitol molecules, as was reported in co-lyophilization of disaccharides with the phosphate salts.<sup>26</sup>

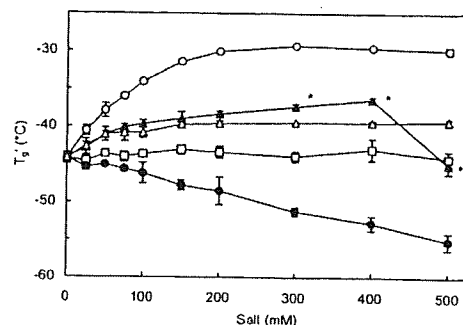


Fig. 5. Effect of Co-solutes on  $T'_g$  of Frozen Sorbitol (500 mM) Solutions. An aliquot of solution ( $10\ \mu\text{l}$ ) in aluminum cell was scanned from  $-70^\circ\text{C}$  at  $5^\circ\text{C}/\text{min}$ . Symbols represent measured midpoint values  $\pm$  S.D. ( $n=3$ ,  $\circ$ :  $\text{Na}_3\text{PO}_4$ ,  $\blacktriangle$ :  $\text{Na}_2\text{HPO}_4$ ,  $\triangle$ : trisodium citrate,  $\square$ :  $\text{NaH}_2\text{PO}_4$ ,  $\bullet$ :  $\text{NaCl}$ ).

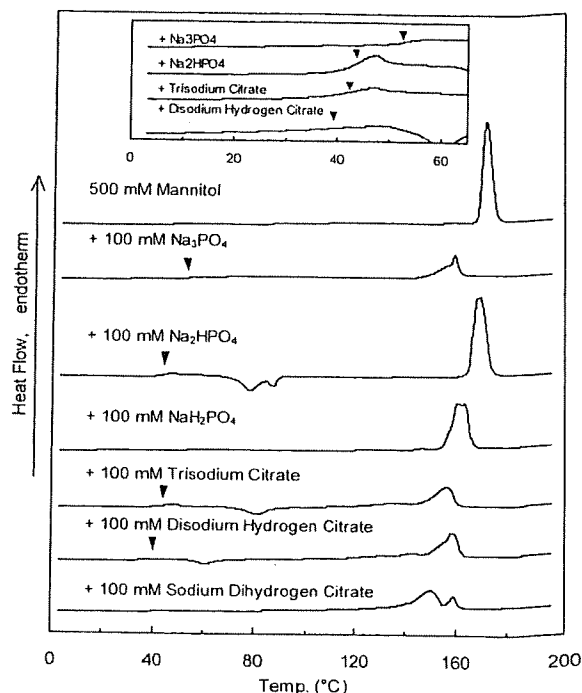


Fig. 6. Thermal Profiles of Freeze-Dried Solids Obtained from Initial Solutions Containing Mannitol (500 mM) and Various Co-solutes (100 mM). Some thermograms were magnified to indicate the glass transition temperatures of the solids ( $\nabla$ ).

Thermal and near-infrared analyses of cooled-melt amorphous sorbitol solids were performed to study the possible salt-induced changes in molecular interactions. A thermogram of cooled-melt sorbitol solid, and effects of the salts on the glass transition temperature ( $T_g$ :  $-1.1^\circ\text{C}$ ) are shown in Fig. 7. The amorphous sorbitol solid showed only a glass transition in the thermal scan up to  $125^\circ\text{C}$ . Trisodium phosphate and citrate exhibited much larger effect to raise the  $T_g$  of the amorphous sorbitol solid than  $\text{Na}_2\text{HPO}_4$  and  $\text{NaCl}$ , suggesting significant reduction in the molecular mobility. Near-infrared spectra of the cooled-melt amorphous sorbitol solid showed several broad bands that indicate random molecular configurations (Fig. 8). The bands in the  $6000$  to  $7000\text{ cm}^{-1}$  range have been assigned as O–H stretch first overtones of hydroxyl groups with intermolecular (around  $6350\text{ cm}^{-1}$ ) and intramolecular (around  $6800\text{ cm}^{-1}$ ) hydro-

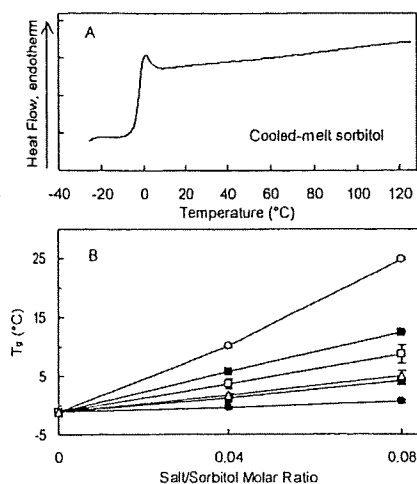


Fig. 7. Thermal Profile (A) and Glass Transition Temperatures (B) of Cooled-Melt Sorbitol-Salt Mixture Solids

Symbols represent measured midpoint  $T_g$  values  $\pm$  S.D. ( $n=3$ , O:  $\text{Na}_3\text{PO}_4$ ,  $\blacktriangle$ :  $\text{Na}_2\text{HPO}_4$ ,  $\blacksquare$ : trisodium citrate,  $\square$ : disodium citrate,  $\triangle$ : monosodium citrate,  $\bullet$ : NaCl).

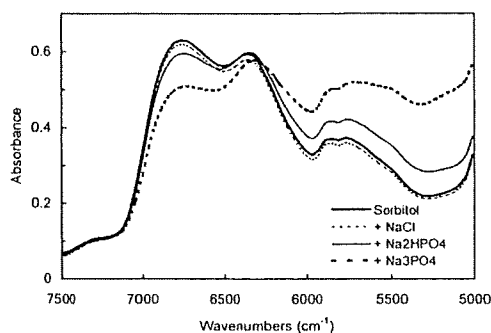


Fig. 8. Transmission Near-Infrared Spectra of Cooled-Melt Solids Containing Sorbitol and Salts ( $\text{Na}_3\text{PO}_4$ ,  $\text{Na}_2\text{HPO}_4$ , NaCl) in the Molar Ratio of 12.5:1

gen-bonding.<sup>34,35</sup> Addition of  $\text{Na}_3\text{PO}_4$  reduced intensity of the band at  $6800\text{ cm}^{-1}$  with concomitant increase in the bands below  $6350\text{ cm}^{-1}$ , suggesting increased intermolecular hydrogen-bonding in the solid. The intense molecular interaction should result in the higher transition temperatures. Absorbance by the phosphate salts should also contribute to the increased intensity in the lower wavenumber region ( $5500\text{--}6000\text{ cm}^{-1}$ ).<sup>34,35</sup> Partial crystallization of cooled-melt mannitol made the solid inappropriate for the NIR study.

### Discussions

Various co-solutes, including popular excipients in pharmaceutical formulations, kinetically and/or thermodynamically prevented the crystallization of mannitol in frozen solutions at certain concentrations. Trisodium and tripotassium phosphates or citrates showed larger effect to prevent the mannitol crystallization in the frozen solutions and freeze-dried solids. The sorbitol and salt combinations indicated reduced mobility of molecules by intense hydrogen-bonding in the freeze-concentrated phase, which should contribute to retain mannitol in the amorphous state.

Miscibility of mannitol and co-solutes in the concentrated fraction should be the first requisite to prevent the mannitol

crystallization in frozen solutions. Mannitol and the various co-solutes were freeze-concentrated into the same phase at certain concentration ratios, and under this condition mixing should kinetically perturb the spatial rearrangement of mannitol molecules required for crystallization. Reported significant melt miscibility of mannitol and some salts (e.g., NaCl) at elevated temperatures suggested their thermodynamic compatibility in the concentrated mixture phase in frozen solutions.<sup>9</sup> On the other hand, thermodynamic solute immiscibility and/or co-solute crystallization (e.g.,  $\text{Na}_2\text{HPO}_4$ ) at above their critical mixing co-solute/mannitol concentration ratios should separate the solutes to different phases in a frozen solution.<sup>36</sup> The co-solute crystallization should induce crystallization of the remaining mannitol molecules. Various factors, including the structure, ionized state and concentrations of co-solutes, as well as the thermal process, should determine the miscibility with mannitol in the frozen solutions.

Reduction of the molecular mobility of mannitol should be another significant requirement to prevent its crystallization in frozen solutions. The upward shift of the transition temperatures ( $T_g$ 's) in the presence of some phosphate and citrate salts should indicate the reduced molecular mobility in the freeze-concentrated phases. Some of the combinations showed their highest  $T_g$ 's at certain salt concentrations, which suggested direct interaction between mannitol and co-solute ions and/or altered molecular interactions between mannitol molecules rather than simple mixing.<sup>23,24</sup> It is plausible that the salt-induced intense intermolecular hydrogen-bonding observed in the cooled-melt sorbitol system also contributes to prevent mannitol crystallization in frozen solution and freeze-dried solids. The different effects of phosphate and citrate salts suggested that ionic valence and local pH are the significant factors involved in altering the molecular interactions. The effect of pH on the molecular interaction between polyols are subject to debate, and will require further study.<sup>26,37</sup>

### References

- Hancock B. C., Zografi G., *J. Pharm. Sci.*, **86**, 1–12 (1997).
- Craig D. Q., Royall P. G., Kett V. L., Hopton M. L., *Int. J. Pharm.*, **179**, 179–207 (1999).
- Izutsu K., Yoshioka S., Terao T., *Chem. Pharm. Bull.*, **42**, 5–8 (1994).
- Pikal M. J., Dellerman K. M., Roy M. L., Riggan R. M., *Pharm. Res.*, **8**, 427–436 (1991).
- Chang B. S., Randall C., *Cryobiology*, **29**, 632–656 (1992).
- MacKenzie A. P., *Phil. Trans. R. Soc. Lond. B.*, **278**, 167–189 (1971).
- Suzuki T., Franks F., *J. Chem. Soc., Faraday Trans.*, **89**, 3283–3288 (1993).
- Kim A. I., Akers M. J., Nail S. L., *J. Pharm. Sci.*, **87**, 931–935 (1998).
- Telang C., Suryanarayanan R., Yu L., *Pharm. Res.*, **20**, 1939–1945 (2003).
- Tong P., Taylor L. S., Zografi G., *Pharm. Res.*, **19**, 649–654 (2002).
- Izutsu K., Fujimaki Y., Kuwabara A., Aoyagi N., *Int. J. Pharm.*, **301**, 161–169 (2005).
- Nail S. L., Jiang S., Chongprasert S., Knopp S. A., *Pharm. Biotechnol.*, **14**, 281–360 (2002).
- Cannon A. J., Trappier E. H., *PDA J. Pharm. Sci. Technol.*, **54**, 13–22 (2000).
- Yu L., Milton N., Groleau E. G., Mishra D. S., Vansickle R. E., *J. Pharm. Sci.*, **88**, 196–198 (1999).
- Lu Q., Zografi G., *Pharm. Res.*, **15**, 1202–1206 (1998).
- Williams N. A., Guglielmo J., *J. Parenter. Sci. Technol.*, **47**, 119–123 (1993).
- Pyne A., Surana R., Suryanarayanan R., *Pharm. Res.*, **19**, 901–908

- (2002).
- 18) Kett V. L., Fitzpatrick S., Cooper B., Craig D. Q., *J. Pharm. Sci.*, **92**, 1919—1929 (2003).
  - 19) Martini A., Kume S., Crivellente M., Artico R., *PDA J. Pharm. Sci. Technol.*, **51**, 62—67 (1997).
  - 20) Johnson R. E., Kirchoff C. F., Caud H. T., *J. Pharm. Sci.*, **91**, 914—922 (2002).
  - 21) Lueckel B., Bodmer D., Helk B., Leuenberger H., *Pharm. Dev. Technol.*, **3**, 325—336 (1998).
  - 22) Telang C., Yu L., Suryanarayanan R., *Pharm. Res.*, **20**, 660—667 (2003).
  - 23) Miller D. P., Anderson R. E., de Pablo J. J., *Pharm. Res.*, **15**, 1215—1221 (1998).
  - 24) Izutsu K., Ocheda S. O., Aoyagi N., Kojima S., *Int. J. Pharm.*, **273**, 85—93 (2004).
  - 25) Yoshinari T., Forbes R. T., York P., Kawashima Y., *Int. J. Pharm.*, **258**, 109—120 (2003).
  - 26) Ohtake S., Schebor C., Palecek S. P., de Pablo J. J., *Pharm. Res.*, **21**, 1615—1621 (2004).
  - 27) Kets E. P. W., IJpelaar P. J., Hoekstra F. A., Vromans H., *Cryobiology*, **48**, 46—54 (2004).
  - 28) Cavatur R. K., Vemuri N. M., Pyne A., Chrzan Z., Toledo-Velasquez D., Suryanarayanan R., *Pharm. Res.*, **19**, 894—900 (2002).
  - 29) Lu Q., Zografi G., *J. Pharm. Sci.*, **86**, 1374—1378 (1997).
  - 30) Murase N., Franks F., *Biophys. Chem.*, **34**, 293—300 (1989).
  - 31) Deluca P., Lachman L., *J. Pharm. Sci.*, **54**, 617—624 (1965).
  - 32) Burger A., Henck J. O., Hetz S., Rollinger J. M., Weissnicht A. A., Stottner H., *J. Pharm. Sci.*, **89**, 457—469 (2000).
  - 33) Yu L., Mishra D. S., Rigsbee D. R., *J. Pharm. Sci.*, **87**, 774—777 (1998).
  - 34) Ozaki Y., Kawata S., "Near-Infrared Spectroscopy," Japan Scientific Societies Press, Tokyo, 1996.
  - 35) Shenk J. S., Workman J. J., Jr., Westerhaus M. O., "Handbook of Near-Infrared Analysis," ed. by Burns D. A., Ciurczak W. W., Taylor & Francis, New York, 2001, pp. 419—474.
  - 36) Randolph T. W., *J. Pharm. Sci.*, **86**, 1198—1203 (1997).
  - 37) Eriksson J. H., Hinrichs W. L., de Jong G. J., Somsen G. W., Frijlink H. W., *Pharm. Res.*, **20**, 1437—1443 (2003).

平成 17 年度「日本薬局方の試験法に関する研究」研究報告\*\*

—皮膚適用製剤の溶出試験に関する研究—

四方田千佳子, 保立 仁美, 伊豆津健一, 青柳 伸男\*

医薬品研究 Vol.38, No.5 別刷 (2007年)

財団法人 日本公定書協会

## 平成 17 年度「日本薬局方の試験法に関する研究」研究報告\*\*

## —皮膚適用製剤の溶出試験に関する研究—

四方田千佳子, 保立 仁美, 伊豆津健一, 青柳 伸男\*

## 1. はじめに

皮膚適用製剤は、皮膚への作用を目的とした局所製剤の他、経口投与でバイオアベイラビリティが低い医薬品等の注射剤に変わる剤形としても広く検討されている。

現在、欧州薬局方 (EP) や米国薬局方 (USP) には、皮膚適用製剤の品質評価法として溶出試験のベッセル内に製剤を固定する装置を設置する方法、パドル部分を改変した溶出試験法等が数種収載されている。しかし、日本薬局方 (日局) では、皮膚適用製剤の品質評価法を収載しておらず、本研究では、これらの試験法に関する研究を実施し、日局への適切な取り込みを目指すこととした。

既に、森本ら<sup>1-3)</sup>は、パドルオーバーディスク法の製剤への適用を検討し、人口汗を試験液として用いると、製剤の膨潤が防げることを示している<sup>2-3)</sup>。また、Shah らは、クロニジン<sup>4)</sup>及びニトログリセリン経皮吸収製剤<sup>5)</sup>に、FDA の推奨する時計皿にテフロンメッシュを組み合わせた器具を使用するパドル法を適用し、製剤のバッチ間の品質管理に有効であることを示している。

USP, EP では数種の方法が並列に並べられており、日局に取り込むにあたってはそれらの整理が必要と考えられた。そこで、本報では、フェルピナク製剤をモデルとして、各試験法や試験条件の影響を詳細に検討し、本質的な因子を明らかにすることを試みた。

## 2. 実験条件

## 2.1 試験製剤

皮膚適用製剤としてフェルピナク貼付剤を取り上げ、市販のもの及び供与されたもの合わせて 8 種を使用した。8 製剤のうち、7 製剤はフェルピナク 70 mg を含有する貼付剤で、1 製剤のみ半分のサイズに 35 mg 含有していた。また、4 製剤は、ポリアクリル酸などを基材とする含水ゲル様の製剤、その他の 4 製剤は、メタクリル酸・アクリル酸 *n*-ブチルコポリマーやスチレン・イソブチレン・スチレンブロック共重合体等を基材とする固い高分子層からなるテープ状の製剤であった。

## 2.2 溶出試験実験条件

溶出試験器は富山産業(株)製、NTR-6100 にオートサンプラー-W を接続し、特に記載しない場合は、試験液には pH 6.0 のリン酸緩衝液 900 mL を用い、32°C、パドル法 50 回転で試験を行った。各試験液採取時間に試験液を 5 mL ずつ分注した。製剤の固定には、USP Apparatus 5 に収載されているパドルオーバーディスク用ディスクに準拠して作成されている富山産業(株)製のものをを使用した。USP Apparatus 6 のシリンダーは富山産業(株)製のものをを用いた。また、膜の特性の影響を見るため、ミリポア製の 47 mm メンブランフィルター膜を装着できる Hanson Research 社製の軟膏用セルを使用した。座剤溶出試験装置として、PHARMA・TEST 社製のものを、拡散セルは Hanson Research 社製のものをを使用した。

\* 国立医薬品食品衛生研究所薬品部 東京都世田谷区上用賀 1-18-1 (〒158-8501)

\*\* 本研究は、平成 17 年度日本公定書協会の「日本薬局方の試験法に関する研究」により行ったものである。

### 2.3 メンブランフィルター

ミリポア社製のセルロース混合エステル (HA), ナイロンメンブレンフィルター (HN), オムニポアメンブレンフィルター (JH), 親水性デュラポアフィルター (HVLP), 疎水性デュラポアフィルター (HVHP) を使用した。

製剤をメンブランフィルターに挟み込み, ヒートシールで接着する場合には, メンブランフィルターは 293 mm 径のものから切り取り, 溶着型ヒートシールは, 白光製製のシール幅 1.6 mm のものを使用した。

### 2.4 溶出試験液中のフェルビナク含量の測定

採取試験液中のフェルビナク含量は HPLC により測定した。HPLC 装置は, Agilent 1100 シリーズ, カラムは, 関東化学製 MightysilRP-18 GP150 (4.6 × 150 mm), 移動相はリン酸 (1→1000) : アセトニトリル = 1 : 1, 検出波長は 254 nm とし, 流速 1 mL/min で試験を行った。

## 3. 実験結果

### 3.1 バドルオーバーディスクによる溶出試験

FDA の推奨する時計皿法及び USP, EP のバドルオーバーディスク法は, いずれもバドルの下に製剤を置いて試験を行う, 溶出試験器を応用した簡便法で, 最も実用性に富むと思われる。そこで, まず, 製剤をそのまま試験液に浸して試験を試みた。

#### 3.1.1 8種製剤の放出挙動

各製剤をそのまま 4 cm 角に切り, バドルオーバーディスク用ステンレス製メッシュに両面テープで貼り付けてベッセル内のリン酸緩衝液 (pH 6.0) 900 mL の底部に沈め, USP, EP の記載に従って, バドルの位置をディスク上 2.5 cm に調整後, 50 回転で試験を行った。8 種の製剤の放出挙動を Fig. 1 に示した。8 種製剤のうち, A~D は含水ゲル様製剤, E~H はテープ様の製剤である。製剤 2 種ずつが類似の挙動を示し, それぞれの処方も類似していた。見かけの類似しているテープ様製剤でも, F, G の製剤では溶出が速く, E, H では溶出が頭打ちとなるなど大きな差が認められた。6 回の試験の標準偏差は小さく, 試験の再現性は良好であった。それぞれの製剤は, 試験終了時まで緩衝液中で構造を維持していたが, 溶出の速い製剤程, 水分を吸収し, 膨潤する傾向が強くと, 通常の製剤適用時とは異なる

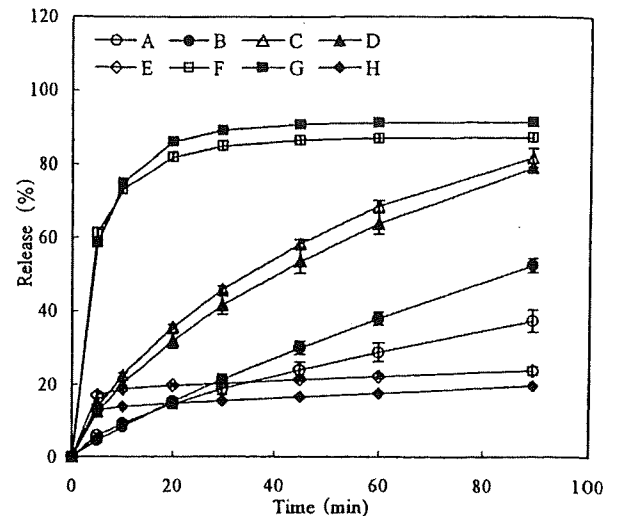


Fig. 1 Release Profiles of Felbinac from 8 Kinds of Patch by Paddle over Disk Method at 50 rpm in 900 mL Phosphate Buffer (pH 6.0) at 32°C (n=6)

状態での溶出挙動であると思われた。

#### 3.1.2 薬物放出への回転数の影響

バドル法での基本回転数の影響を溶出の速い状況で検討した。製剤 C と製剤 H の 2 種について, 回転数を 50 回転から 100 回転へ上げて, 溶出挙動を比較した。Fig. 2 に示すように, 製剤 H では, 溶出挙動に全く差は認められず, 製剤 C でもその差は大きくなかった。回転数は, 攪拌力により製剤の

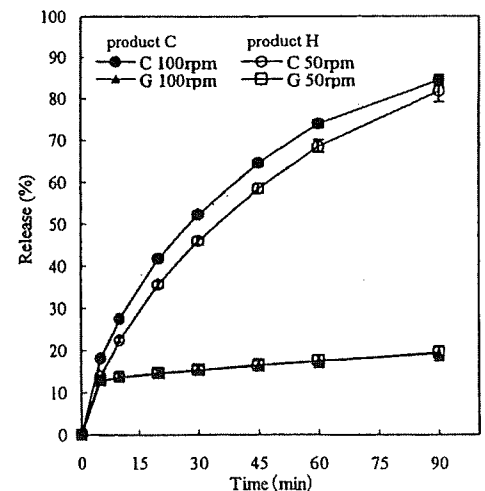


Fig. 2 Effect of Paddle Rotation Speed to the Release of Felbinac from Two Kinds of Patches (product C, product H) (n=3)

崩壊を起こす必要はなく、医薬品の拡散層が混合されれば良く、50回転で十分と考えられた。以後の試験では、すべて50回転で実施した。

### 3.2 メンブランフィルター使用の検討

皮膚適用製剤の溶出試験では、従来から、製剤が直接試験液に接しないようにする目的で、試験液と製剤を隔てるために透析膜やメンブランフィルターが使用されてきた<sup>9)</sup>。Fig. 1の溶出試験では、製剤によってはゲル部分の吸水が大きく、薬物保持層の状態が通常の貼付状態とかけ離れていると思われる変化が認められた。そこで、製剤をメンブランフィルターに貼り付けて試験液と接触させることにより、製剤の大きさや表面積を固定した上で、種々の試験条件と放出性の関係を検討することとした。

#### 3.2.1 メンブランフィルターの材質の影響

従来、メンブランフィルターを使用すると、膜の特性によって薬物の放出が変わるという報告が多々見られるが、膜の孔径が決して小さくなく、膜の特性により医薬品の透過性の差は、膜孔の濡れやすさのみに依存するのではと考えた。そこで、まず、メンブランフィルターを乾いたまま製剤の上に貼り付けて試験を行い、次に、あらかじめ試験液を通して十分に膜孔を濡らして同様の試験を実施することとした。軟膏用セルに、各製剤を粘着層を上側にして両面テープで貼り付け、その上に孔径0.45  $\mu\text{m}$ 、47

mm径のメンブランフィルターを置き、膜を押さえるリングを締め付けて、ベッセル底部に沈め、パドル法で試験を行った。特に疎水性の強いHVHP膜では、試験液を通じる際には、まずメタノールを通し、次いで試験液を通してから、試験を実施した。

Fig. 3に含水ゲル様の製剤Cにおける結果を示した。製剤Cでは、膜を使用しないFig. 1の挙動と比較すると全体的に放出が遅くなり、メンブランフィルターを介して試験液に接触することにより、製剤の膨潤の程度が小さくなり、製剤のゲル状態をより維持できるためと考えられる。ここで検討したメンブランフィルターのうち、疎水性の強いHVHP膜では、そのまま使用すると全くフェルビナクを放出しなかったが (Fig. 3(A))、メタノールで湿潤させると、その他の膜と同様に薬物の放出が見られた (Fig. 3(B))。含水ゲル様の製剤でも、テープ様の製剤でも、そのまま膜を使用した場合よりも、膜を試験液で湿潤させると、膜間での放出性の差は小さくなり、膜による薬物の放出の差は、膜の試験液中での濡れ特性の差に起因することが示唆された。

#### 3.2.2 メンブランフィルターの孔径の影響

HA膜の、孔径0.025  $\mu\text{m}$ 、0.1  $\mu\text{m}$ 、0.45  $\mu\text{m}$ の3種の膜を用い、フェルビナク放出に及ぼす孔径の影響について検討した。Fig. 5に示すように、孔径の小さな膜はそのまま使用すると膜孔が濡れにくく

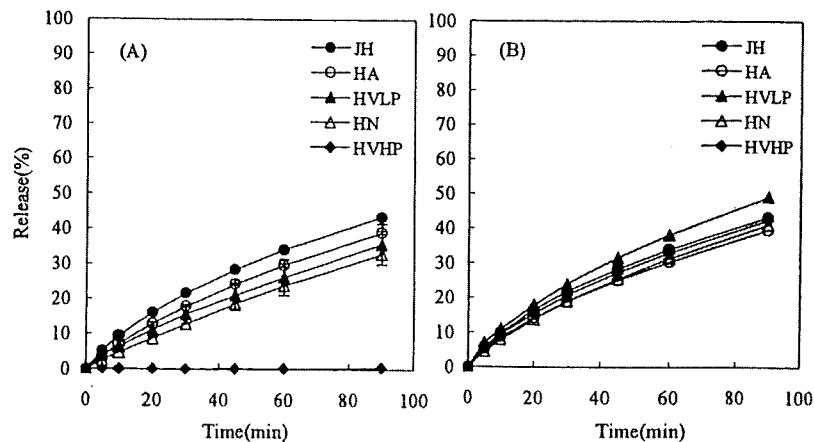


Fig. 3 Effect of Material of Membrane Filter to the Release of Felbinac from Product C (n=2)

(A) Without pretreatment of membrane. (B) All membranes were pre-wetted by the filtration of test solution.

Materials; JH: Polytetrafluoroethylene, HA: Cellulose acetate, HVLP: Polyvinylidene fluoride, HN: Nylon, HVHP: Hydrophobic polyvinylidene fluoride

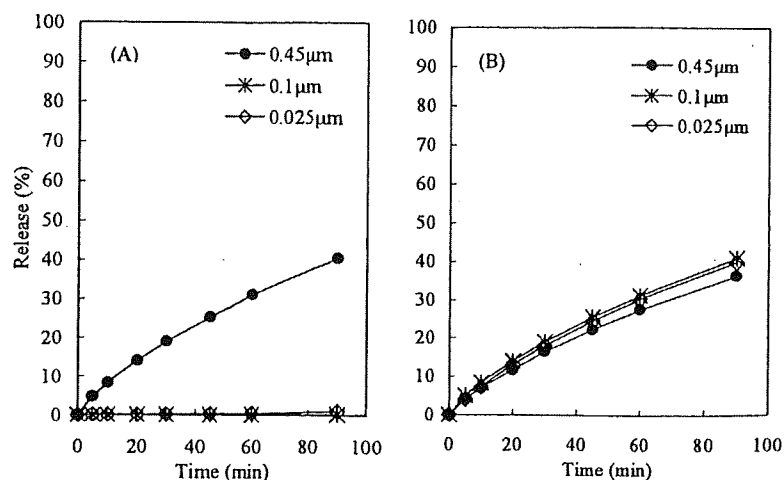


Fig. 4 Effect of the Pore Size of HVLP Membrane to the Release of Felbinac from Product C (n=1)

(A) Without pretreatment of membrane. (B) All membrane were pre-wetted by the filtration of test solution.

医薬品を透過しないが (Fig. 4(A)), 膜にあらかじめ試験液を通過させておくと, 孔径にかかわらず薬物を放出することが示された (Fig. 4(B)). これらの結果から, メンブランフィルターのような分子ふるい効果の無い比較的孔の大きな膜では, 膜孔のぬれのみを気に付ければ, 膜孔の大きさが薬物の透過性を制御するものではないと考えられる.

さらに, テープ状の製剤で, 試験液と直接接触してもほとんど膨潤せず堅い高分子層を持つ製剤である H について Fig. 4, 5 と同様の試験を実施したところ, 同様に膜の材質, 孔径の影響は受けないことが示された. また, 製剤 H では, 膜の有無に関わらず, Fig. 1 と放出挙動に変化は認められなかった. したがって, 製剤 C におけるメンブランフィルターを介したことによる放出率の減少は, 製剤側の薬物保持状態の変化によるものであり, 膜の存在が薬物の透過を妨げることに依るものではないと考えられる.

これらの結果から, 以後の検討では, 比較的柔軟性に富む HVLP 膜の汎用孔径  $0.45 \mu\text{m}$  のものを使用することとした.

### 3.2.3 パドルと製剤間の距離の影響

USP, EP では, パドルオーバーディスク法では, 製剤とパドル底部の距離を, 経口固形製剤での, ベッセル底部からの距離と同様に  $2.5 \text{ cm}$  とするよう規定している. しかし, 皮膚適用製剤の場合には,

水流による製剤の崩壊への影響も無く, 単に医薬品の拡散層が適切に攪拌されれば良いのではと考えられたため, パドルと製剤間の距離を  $1.5 \text{ cm}$ ,  $2.5 \text{ cm}$ ,  $3.5 \text{ cm}$  の三段階に変化させて, 製剤 C 及び製剤 H につき, 試験を行った. Fig. 5 に示すように, パドルと製剤間の距離が変化しても, フェルビナクの放出に大きな差は認められず, 必ずしも  $2.5 \text{ cm}$  と規定する必然性は認められない. 溶出試験器によっては, パドルの位置の変更が困難な場合も少なくなく,

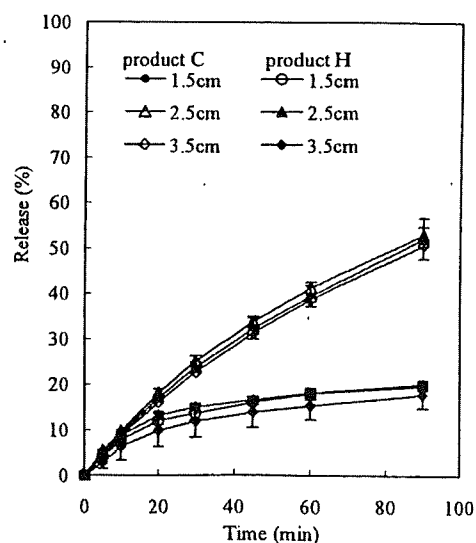


Fig. 5 Effect of the Distance between Paddle and Patch to the Release of Felbinac (n=3)



通常のパドル位置で底部に沈めることも可能と考えられる。

3.2.4 他の試験装置との比較

USP, EP ではパドル法の別法として、パドル部分の代わりに、シリンダーと呼ばれる円筒型の金属製装置を取り付ける試験法が記載されている。そこで、製剤 C を用いて、パドルオーバーディスク法とシリンダー法の溶出挙動の比較を試みた。Fig. 6 の右側に示すようなシリンダーに 4 cm 角に切った製剤 C をそのまま、あるいは、HVLP 膜で挟んで 4 辺をヒートシールしたものを両面テープで貼り付けて、試験を実施したところ、膜の有無に関わらず、シリンダーで試験液中で回転させても、ベッセル底部に沈めた場合と溶出性にほとんど差は認められなかった (Fig. 6)。したがって、特にシリンダーを使用しなくても、簡便なパドル法で十分と思われた。

同じようにメンブランフィルターを使用し、溶出試験器を用いる座薬放出試験用装置及び拡散セルを使用して放出性の比較を試みた。

座薬放出試験用装置では、製剤 C 及び製剤 H につき、溶出試験と同サイズの製剤を HVLP 膜に貼り付けて膜を筒状にして装置に装着して試験を試みたところ、製剤を単に底面に沈めた場合と放出性に差は認められなかった。

また、拡散セルに HVLP 膜をセットし、孔径よりやや小さめの製剤を膜面に貼り付けて試験を行ったところ、放出率はパドルオーバーディスク法とほぼ類似した結果を与えた。したがって、皮膚適用製剤の溶出試験では、試験中の製剤薬物層の状態を制御し、試験液中の薬物濃度を均一にすることが、一連の試験法の共通因子であり、どのように配置するか、製剤を回転するか等その他の条件はあまり重要ではないと思われた。製剤の大きさがフレキシブルであること、装置の汎用性の面からも、皮膚適用製剤では、パドル法による試験の採用が妥当と考えられた。

3.2.5 8 種製剤における HVLP 膜を用いた溶出試験

軟膏容器を使用すると、製剤の膨潤が起こる場合には、製剤が枠から抜け出る事例が認められた。そこで、特殊な装置を用いることなく、製剤をメンブランフィルターに貼り付ける方法として、Fig. 6 でも試みたように、製剤よりやや大きなメンブランフィルターで製剤を挟み、4 辺をヒートシールで接着して溶出試験を実施した。Fig. 1 と同様の 8 種製剤での結果を、Fig. 7 に示した。メンブランフィルターを使用した場合、製剤は放出面のみが膜孔から試験液に接するため、製剤の形状が大きく変化することなく放出試験の実施が可能であった。Fig. 1 と

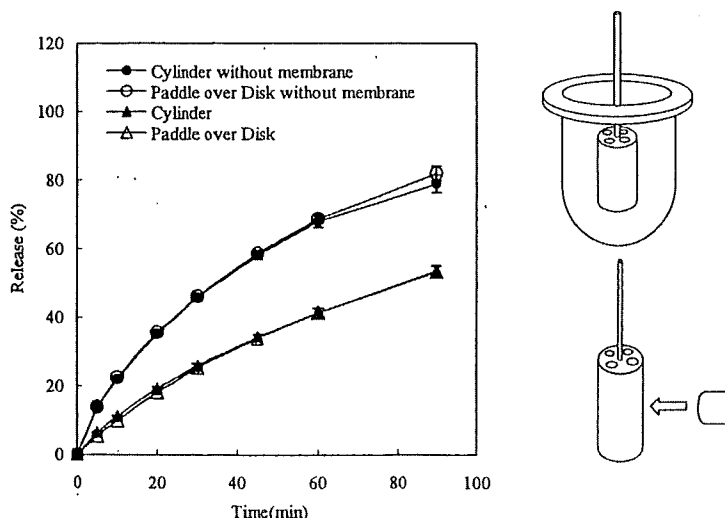


Fig. 6 Comparison of Release Profile of Felbinac from Product C between the Apparatus of Cylinder and Paddle over Disk (n=3) Cylinder is illustrated in the right side.

比較すると、製剤 E、製剤 H では、膜の有無がほとんど影響していない。これは、両製剤は固いテープ状であり、試験液による製剤側の変化が小さいためであろう。また、この 2 種の製剤のみで、放出が 1 時間程度で頭打ちとなる傾向が見られ、製剤の表面に近い部分が容易に放出されると思われる。同じテープ状の製剤でも、製剤 F や製剤 G では、膜を介することで大きく放出率が低下した。これは、テープ剤でも成分によっては含水傾向があり、水による構造変化が大きい場合があることを示している。その他のゲル様の製剤では、ほぼ、直線的な放出挙動を示し、同じ処方製剤の品質試験には充分使用できると思われた。

#### 4. 考 察

本研究では、皮膚適用製剤の溶出試験の日局への収載を目指し、試験の本質的な要因を明らかにすることを試みると共に、パドル法による皮膚適用製剤の放出試験で、メンブランフィルターを製剤に簡便に装着する方法を提案した。

フェルビナク貼付剤をモデル製剤として検討した結果、製剤をそのまま、あるいは適切な膜に挟み込み、重りに貼付してベッセル底部に沈めたパドル法による試験が、他の装置による試験とほぼ同等の結果を与え、簡便で有効な方法であると考えられた。

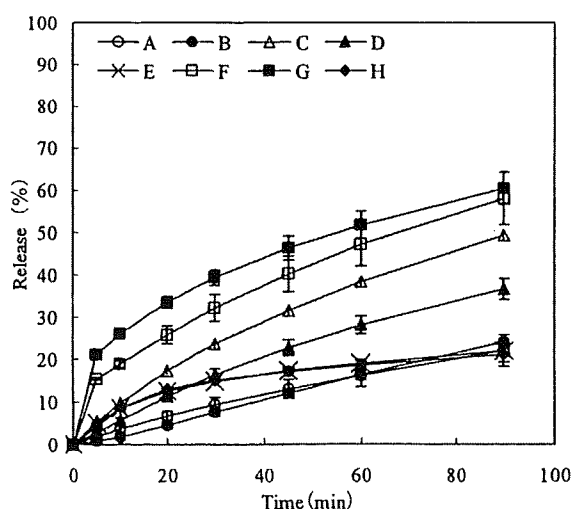


Fig. 7 Release Profiles of Felbinac from 8 Kinds of Patches by Paddle over Disk Method Using HVLP Membrane at 50 rpm in 900 mL Phosphate Buffer (pH 6.0) at 32°C (n=6)

製剤を沈めるための重りとしては、USP の例示のようなディスクも使用できるが、金属製であるためベッセルを傷つけることがあるため、ベッセルの硝子を傷つけない、なるべくなめらかな素材が望まれる。

また、本報では製剤を試験液と隔てるためにメンブランフィルターを使用した。原薬や製剤の特性に応じて、ヒートシール可能な他の膜も使用可能である。

なお、本法では、フェルビナクは比較的中性領域の緩衝液に溶解しやすいため問題はなかったが、皮膚表面の pH である pH 5~6 の緩衝液で放出しにくい医薬品では、pH を変化させるか、数十%のアルコール溶液、界面活性剤等の使用も検討する必要がある。その場合、試験液による製剤側の変化、膜の劣化に留意する必要がある。フェルビナク製剤で、膜を使用せずに試験液を変えた場合の溶出例を Fig. 8 に示した。フェルビナクの pKa は 3.9 であるため、pH 4.0 ではいずれの製剤もあまり放出しないが、アルコールでは溶解性が高くなるため、放出が速い。このように、製剤からの放出は試験液の組成により大きく変わる。

フェルビナクを単位面積当たり同じ量を含む製剤でも、製剤の処方によって放出性が異なること、膜を使用した場合と、使用しない場合の放出挙動の差も、製剤により異なることが示された。

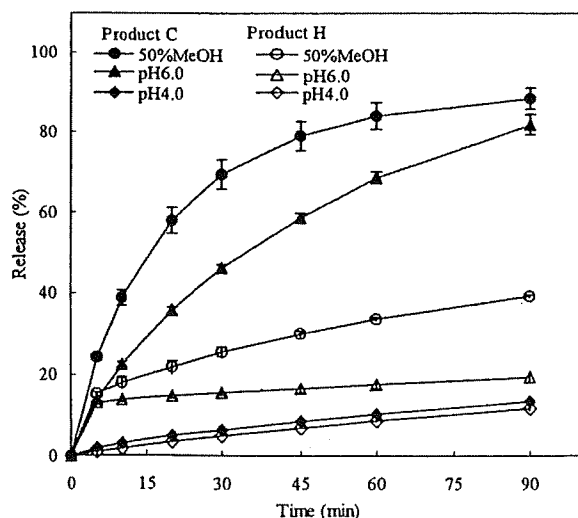


Fig. 8 Effect of the Test Solution to the Release of Felbinac (n=3)

皮膚適用製剤の放出試験は、試験液に曝され、受け側が水溶液であるなど、必ずしも適用時の皮膚表面での放出性を再現するものではないため、放出性の差が、直接、製剤の有効性の指標となるものではない。個々の製剤の品質特性を捉え、品質の管理に有効な試験法と位置づけられるものである。

#### 謝 辞

試験用製剤を御供与下さいました、外用製剤協議会に深謝致します。

#### 文 献

- 1) 森本雍憲, 小林大介, 夏目秀視, 沼尻幸彦: 医薬品研究, 30(00), 556-558 (1999).
- 2) 平船寛彦, 島村剛史, 上田秀雄, 沼尻幸彦, 小林大介, 森本雍憲: 医療薬学, 30(00), 723-729 (2004).
- 3) Shimamura, T., Tairabune, T., Kogo, T., Ueda, H., Numajiri, S., Kobayashi, D., Morimoto, Y.: *Chem. Pharm. Bull.*, 52, 167-171 (2004).
- 4) Shah, V. P., Tymes, N. W., Skelly, A. P.: *Pharm. Res.*, 6, 346-351 (1989).
- 5) Shah, V. P., Lesko L. J., Williams, R. L.: *Eur. J. Pharm. Biopharm.*, 41, 163-167 (1995).
- 6) Shah, V. P., Elkins, J., Hanus, J., Noorizadeh, C., Skelly, J. P.: *Pharm. Res.*, 8, 55-59 (1991).

1) 森本雍憲, 小林大介, 夏目秀視, 沼尻幸彦: 医

# ファルマシア

別刷